Mixed Efficient Global Optimization for Time-Dependent Reliability Analysis

Zhen Hu
Department of Mechanical and Aerospace Engineering,
Missouri University of Science and Technology,
290D Toomey Hall,
400 West 13th Street,
Rolla, MO 65409-0500
e-mail: zh4hd@mst.edu

Xiaoping Du
Professor
Department of Mechanical and Aerospace Engineering,
Missouri University of Science and Technology,
272 Toomey Hall,
400 West 13th Street,
Rolla, MO 65409-0500
e-mail: dux@mst.edu

Time-dependent reliability analysis requires the use of the extreme value of a response. The extreme value function is usually highly nonlinear, and traditional reliability methods, such as the first order reliability method (FORM), may produce large errors. The solution to this problem is using a surrogate model of the extreme response. The objective of this work is to improve the efficiency of building such a surrogate model. A mixed efficient global optimization (m-EGO) method is proposed. Different from the current EGO method, which draws samples of random variables and time independently, the m-EGO method draws samples for the two types of samples simultaneously. The m-EGO method employs the adaptive Kriging–Monte Carlo simulation (AK–MCS) so that high accuracy is also achieved. Then, Monte Carlo simulation (MCS) is applied to calculate the time-dependent reliability based on the surrogate model. Good accuracy and efficiency of the m-EGO method are demonstrated by three examples. [DOI: 10.1115/1.4029520]

Keywords: Kriging, reliability analysis, mixed EGO, time-dependent

1 Introduction

Reliability is defined within a period of time when a limit-state function involves time. For this case, time-independent reliability analysis methodologies [1,2] are not applicable, and time-dependent reliability methods should be used. Even though other methods [3–5] exist for time-dependent reliability problems, the most widely used methods are first-passage methods and extreme value methods. The former methods are easier to implement and are therefore more popular, but may not be as accurate as the latter methods. The two types of methods are briefly reviewed below.

The first-passage methods calculate the probability that the response exceeds its failure threshold (limit state) for the first time in a predefined period of time. The event that the response reaches its limit state is called an upcrossing, and the upcrossing rate is the rate of change in the upcrossing probability with respect to time. If the first-time upcrossing rate is available, the time-dependent probability of failure can be easily computed. But it is difficult to obtain the first-time upcrossing rate. For this reason, approximation methods are widely used. The most commonly used method is the Rice's formula [6], which uses upcrossing rates throughout the entire period of time with the assumption that all the upcrossings are independent.

Many methods have been developed based on the Rice's formula. For instance, an asymptotic outcrossing rate for stationary Gaussian processes was derived by Lindgren [7] and Breitung [8,9]. The bounds of the upcrossing rate of a nonstationary Gaussian process were given by Ditlevsen [10]. To solve general time-dependent reliability problems, Hagen and Tvedt [11,12] proposed a parallel system approach. A PHI2 method was developed by Sudret and coworkers [13]. Hu and Du also developed a time-dependent reliability analysis method based on the Rice's formula [14]. Even if some modifications have been made [15–18], the upcrossing methods may still produce large errors when upcrossings are strongly dependent.

The extreme value methods approximate the time-dependent reliability from another aspect by using the extreme value of the response with respect to time. If the distribution of the extreme value can be accurately estimated, the accuracy of reliability analysis will be higher than the upcrossing rate methods since the independent upcrossing assumption is eliminated. Accurately and efficiently estimating the distribution of the extreme value, however, is a challenge since global optimization with respect to time should be performed repeatedly.

In general, the extreme value of the response is much more nonlinear than the response itself with respect to the input random variables. For some problems, the distribution of the extreme response is multimodal with different modes (peaks of probability density) even though the response itself follows a unimodal distribution [19]. For this reason, using design of experiments (DOE) to obtain a surrogate model of the extreme response becomes promising and practical. For example, Wang and Wang [20] proposed an extreme response method using the efficient global optimization (EGO) approach [21]; Chen and Li [22] studied how to evaluate the distribution of the extreme response using the probability density evolution method [22].

The efficiency of the existing extreme value methods with DOE, such as the approach reported in Ref. [20], can be improved. To show the feasibility of the improvement, we first define the response function as $Y = g(\mathbf{X}, t)$, where $\mathbf{X} = [X_1, X_2, \ldots, X_n]$ is a vector of random variables, t is the time, and Y is a response. In many applications, the response function may be a black box, such a computer-aided engineering model. To obtain the extreme values of Y, current methods draw samples of $\mathbf{X}$ first. Then at each sample point of $\mathbf{X}$, samples of t are drawn through EGO [21], which produces the extreme response with respect to time at each sample point of $\mathbf{X}$. Thus, the values of the extreme response are available at all the sample points of $\mathbf{X}$, and a surrogate model of the extreme response is then built. Sampling on $\mathbf{X}$ and t is performed at two nested and independent levels, and we therefore call the method the *independent EGO method*. The interaction effects of $\mathbf{X}$ and t are not considered at the two separate sampling levels. The efficiency could be improved if $\mathbf{X}$ and t are sampled simultaneously. This motivated us to develop a new method with higher efficiency.

This work develops a new time-dependent reliability method based on EGO and the active learning strategy [23]. The new method is named the mixed-EGO method since $\mathbf{X}$ and t are

Contributed by the Design Automation Committee of ASME for publication in the Journal of Mechanical Design. Manuscript received September 21, 2014; final manuscript received December 14, 2014; published online February 16, 2015. Assoc. Editor: Gary Wang.

sampled simultaneously. The significance of this work consists of the following elements:

- A mixed EGO method: the new method generates samples of $\mathbf{X}$ and t simultaneously so that the interaction effects of $\mathbf{X}$ and t is considered. This requires fewer training points for building surrogate models and therefore increases the efficiency of the EGO method.
- The integration of the mixed-EGO method with the AK–MCS [23]. The integration makes the surrogate model of the extreme response accurate near or at the limit state and hence improves both accuracy and efficiency of the time-dependent reliability analysis.

The remainder of this paper starts from Sec. 2 where EGO and time-dependent reliability are reviewed. The new method is discussed in Sec. 3. Three examples are presented in Sec. 4, and conclusions are given in Sec. 5.

2 Background

EGO is used in this work. We at first review EGO and discuss the definition of time-dependent reliability. We then review the current independent EGO method for time-dependent reliability analysis [24,25].

2.1 EGO. Since being proposed by Jones in 1998 [21], EGO has been widely used in various areas [26–29]. EGO is based on the DACE model [30] or the Kriging model. Both of the models are updated by adding training points gradually, but they use different criteria for model updating. The EGO model is updated with a new training point that maximizes the expected improvement function (EIF) while the DACE model is updated with a new training point that minimizes the mean square error. A maximum EIF helps find a point with the highest probability to produce a better extreme value of the response. Many studies have demonstrated that EGO can significantly reduce the number of training points for global optimization.

EGO at first constructs a Kriging model using initial training points, and the expected improvement (EI) is calculated using the mean and covariance of the Kriging model. The model is then updated by adding a new point with the maximum EI. The procedure continues until convergence is achieved.

The Kriging model $\hat{g}(\mathbf{x})$ is given by

$$\hat{y} = \hat{g}(\mathbf{x}) = \mathbf{h}(\mathbf{x})^{\mathrm{T}}\boldsymbol{\beta} + Z(\mathbf{x}) \tag{1}$$

in which $\mathbf{h}(\cdot)$ is called the trend of the model, $\boldsymbol{\beta}$ is the vector of the trend coefficients, and $Z(\cdot)$ is a stationary Gaussian process with a mean of zero and a covariance given by

$$\mathrm{Cov}[Z(\mathbf{a}), Z(\mathbf{b})] = \sigma_Z^2 R(\mathbf{a}, \mathbf{b}) \tag{2}$$

where σ_Z^2 is the variance of the process, and $R(\mathbf{a}, \mathbf{b})$ is the correlation function. The commonly used correlation functions include the squared-exponential and Gaussian types [30].

At a training point $\mathbf{x}$, $\hat{y}$ is a Gaussian random variable denoted by

$$\hat{y} = \hat{g}(\mathbf{x}) \sim N(\mu(\mathbf{x}), \sigma^2(\mathbf{x})) \tag{3}$$

in which $N(\cdot,\cdot)$ stands for a normal distribution; $\mu(\cdot)$ and $\sigma(\cdot)$ are the mean and standard deviation of $\hat{y}$, respectively. At a training point $\mathbf{x}$, $\mu(\mathbf{x}) = g(\mathbf{x})$ and $\sigma(\mathbf{x}) = 0$, and $\hat{g}(\mathbf{x})$ therefore passes all the points that have been sampled.

For the global maximum of $g(\mathbf{x})$, the improvement is defined by $I = \max(y - y^*, 0)$, where y^* is the current best solution (the maximum response) obtained from all the sampled training points. Its expectation or EI is then computed by [21]

$$\mathrm{EI}(\mathbf{x}) = (\mu(\mathbf{x}) - y^*)\Phi\left(\frac{\mu(\mathbf{x}) - y^*}{\sigma(\mathbf{x})}\right) + \sigma(\mathbf{x})\phi\left(\frac{\mu(\mathbf{x}) - y^*}{\sigma(\mathbf{x})}\right) \tag{4}$$

where $\Phi(\cdot)$ and $\phi(\cdot)$ are the cumulative distribution function and probability density function of a standard Gaussian variable, respectively, and y^* is

$$y^* = \max_{i=1,2,\ldots,k}\{g(\mathbf{x}^{(i)})\} \tag{5}$$

in which k is the number of current training points.

By maximizing EI, we find a new training point.

$$\mathbf{x}^{(k+1)} = \arg\max_{\mathbf{x}\in\mathbf{X}} \mathrm{EI}(\mathbf{x}) \tag{6}$$

Algorithm 1 (Table 1) below describes the procedure of EGO. More details can be found in Refs. [21] and [30].

In Step 3, $\varepsilon_{\mathrm{EI}}$ (a small positive number) is used as a convergence criterion. The maximum EI is scaled in line 7 as suggested in Ref. [19].

2.2 Time-Dependent Reliability. For a general limit-state function $Y = g(\mathbf{X}, t)$, a failure occurs if

$$Y = g(\mathbf{X}, t) \geq e \tag{7}$$

in which e is the failure threshold.

For a time interval $[t_0, t_s]$, the time-dependent reliability is defined by [5]

$$R(t_0, t_s) = \Pr\{Y = g(\mathbf{X}, t) < e, \quad \forall t \in [t_0, t_s]\} \tag{8}$$

where $\Pr\{\cdot\}$ stands for a probability, and $\forall t \in [t_0, t_s]$ means all time instants on $[t_0, t_s]$.

The time-dependent probability of failure is defined by

$$p_f(t_0, t_s) = \Pr\{Y = g(\mathbf{X}, t) \geq e, \quad \exists t \in [t_0, t_s]\} \tag{9}$$

where $\exists$ stands for "there exists."

$p_f(t_0, t_s)$ is a nondecreasing function of the length of $[t_0, t_s]$. The longer is the period of time, the higher is $p_f(t_0, t_s)$ in general.

2.3 Time-Dependent Reliability Analysis With Surrogate Models. The failure event in Eq. (7) is equivalent to $Y_{\max} > e$, where $Y_{\max}$ is the global maximum response on $[t_0, t_s]$ and is given by

$$Y_{\max} = \arg\max_{t\in[t_0,t_s]}\{g(\mathbf{X}, t)\} \tag{10}$$

Table 1 Detailed procedure of Algorithm 1

Algorithm 1: Efficient Global Optimization (EGO)
1 Generate initial samples $\mathbf{x}^s = [\mathbf{x}^{(1)}; \mathbf{x}^{(2)}; \ldots; \mathbf{x}^{(k)}]$
2 Compute $\mathbf{y}^s = [g(\mathbf{x}^{(1)}), g(\mathbf{x}^{(2)}), \ldots, g(\mathbf{x}^{(k)})]$; set $m = 1$
3 **While** $\{m = 1\}$ **or** $\{\max_{\mathbf{x}\in\mathbf{X}} \mathrm{EI}(\mathbf{x}) < \varepsilon_{\mathrm{EI}}\}$ **do**
4 Construct a Kriging model $\hat{y} = \hat{g}(\mathbf{X})$ using $\{\mathbf{x}^s, \mathbf{y}^s\}$
5 Find $y^* = \max_{i=1,2,\ldots,k+m-1}\{g(\mathbf{x}^{(i)})\}$
6 Search for $\mathbf{x}^{(k+m)} = \arg\max_{\mathbf{x}\in\mathbf{X}} \mathrm{EI}(\mathbf{x})$, where $\mathrm{EI}(\mathbf{x})$ is computed by Eq. (4)
7 Scale $\max_{\mathbf{x}\in\mathbf{X}} \mathrm{EI}(\mathbf{x}) = \max_{\mathbf{x}\in\mathbf{X}} \mathrm{EI}(\mathbf{x})/\lvert\beta(1)\rvert$, where $\beta(1)$ is the first element of the trend coefficients $\boldsymbol{\beta}$ given in Eq. (1)
8 Compute $g(\mathbf{x}^{(k+m)})$; update $\mathbf{y}^s = [\mathbf{y}^s, g(\mathbf{x}^{(k+m)})]$ and $\mathbf{x}^s = [\mathbf{x}^s; \mathbf{x}^{(k+m)}]$
9 $m = m + 1$
10 **End While**

Then $p_f(t_0, t_s)$ is rewritten as

$$p_f(t_0, t_s) = \Pr\{Y_{\max}(\mathbf{X}) > e\} \tag{11}$$

For many problems, $Y_{\max}$ is highly nonlinear with respect to $\mathbf{X}$ and may follow a multimodal distribution. Using existing reliability methods, such as the FORM and second order reliability methods (SORM), may result in large errors. MCS becomes a choice if a surrogate model, $Y_{\max} = \hat{g}_{\max}(\mathbf{X})$, of $Y_{\max}$, can be built. As discussed previously, the direct EGO method is employed to solve time-dependent reliability problems by Wang and Wang [20]. The surrogate model of extreme response $Y_{\max} = \hat{g}_{\max}(\mathbf{X})$ was built with a nested procedure. The outer loop generates samples of $\mathbf{X}$ while the inner loop is executed to find the time $t_{\max}$ when the response is maximum. Samples of t are generated by EGO in the inner loop. A more direct and general independent EGO procedure similar to the aforementioned nested procedure [20] is summarized below.

- Outer loop: sampling on $\mathbf{X}$ for building $Y_{\max} = \hat{g}_{\max}(\mathbf{X})$.
- Inner loop: EGO for $y_{\max} = \max\limits_{t \in [t_0, t_s]} \{g(\mathbf{x}, t)\}$ at $\mathbf{x}$, which is a sample of $\mathbf{X}$.

The associated algorithm or Algorithm 2 is shown as follows (Table 2).

In step 3, ε_{MSE} is a small positive number used as the convergence criterion for the mean square error MSE.

The independent EGO method may not be efficient for two reasons. First, the one-dimensional EGO with respect to t is performed repeatedly at each sample point of $\mathbf{X}$. As mentioned previously, $\mathbf{X}$ and t are treated independently at two separate levels, and the interaction of $\mathbf{X}$ and t is therefore ignored. Not considering the interaction effect of $\mathbf{X}$ and t may result in low computational efficiency. Second, a small MSE is expected for an accurate surrogate model for reliability analysis. Constructing a surrogate model with a low MSE, however, is computationally expensive because $Y_{\max}$ is in general highly nonlinear and possibly multimodal.

3 A Mixed-EGO Based Method

In this section, we discuss the mixed-EGO based method that overcomes the drawbacks of the independent EGO method. The new method builds a surrogate model $Y_{\max} = \hat{g}_{\max}(\mathbf{X})$ for the global extreme response through another surrogate model $Y = \hat{g}(\mathbf{X}, t)$. It is efficient because of the following reasons:

- Using $Y = \hat{g}(\mathbf{X}, t)$ can the effectively account for the joint effects of $\mathbf{X}$ and t and will reduce the number of samples of both $\mathbf{X}$ and t.
- The mixed EGO along with the AK–MCS method [23] can efficiently and accurately approximate the extreme response at or near the limit state. High accuracy at or near the limit state will reduce the number of samples of $\mathbf{X}$.

Table 2 Detailed procedure of Algorithm 2

Algorithm 2: Independent EGO method
1 Generate initial samples $\mathbf{x}^s = [\mathbf{x}^{(1)}; \mathbf{x}^{(2)}; \ldots; \mathbf{x}^{(k)}]$
2 Solve for $\mathbf{y}^s_{\max} = [g_{\max}(\mathbf{x}^{(1)}), g_{\max}(\mathbf{x}^{(2)}), \ldots, g_{\max}(\mathbf{x}^{(k)})]$, where $g_{\max}(\mathbf{x}^{(i)}) = \max\limits_{t \in [t_0, t_s]} \{g(\mathbf{x}^{(i)}, t)\}$, using EGO; set $m = 1$
3 **While** $\{m = 1\}$ **or** $\{\max\limits_{\mathbf{x} \in \mathbf{X}} \text{MSE}(\mathbf{x}) < \varepsilon_{\text{MSE}}\}$ **do**
4 Construct a Kriging model $Y_{\max} = \hat{g}_{\max}(\mathbf{X})$ using $\{\mathbf{x}^s, \mathbf{y}^s_{\max}\}$
5 Find $\mathbf{x}^{(k+m)} = \arg \max\limits_{\mathbf{x} \in \mathbf{X}} \{\text{MSE}(\mathbf{x})\}$
6 Search for $g_{\max}(\mathbf{x}^{(k+m)}) = \max\limits_{t \in [t_0, t_s]} \{g(\mathbf{x}^{(k+m)}, t)\}$ using EGO
7 Update $\mathbf{x}^s = [\mathbf{x}^s; \mathbf{x}^{(k+m)}]$ and $\mathbf{y}^s_{\max} = [\mathbf{y}^s_{\max}, g_{\max}(\mathbf{x}^{(k+m)})]$
8 $m = m + 1$
9 **End While**
10 Reliability analysis using $Y_{\max} = \hat{g}_{\max}(\mathbf{X})$

3.1 Overview. As discussed in Ref. [19], the accuracy of reliability analysis is determined by only the accuracy of the surrogate model at the limit state or $Y_{\max} = g_{\max}(\mathbf{X}) = e$. For this reason, we focus on achieving high accuracy of $Y_{\max} = \hat{g}_{\max}(\mathbf{X})$ at or near the limit state. By doing so, the number of samples can be reduced. Since the limit-state $Y_{\max} = g_{\max}(\mathbf{X}) = e$ is of the greatest concern, the sample updating criterion needs to be modified. In this work, we integrate the AK–MCS method [23] with the proposed mixed-EGO method.

The overall procedure of the mixed-EGO based method is provided in Table 3, and the detailed algorithm will be discussed in Secs. 3.3 and 3.4 and will be summarized in Sec. 3.5.

The major difference between the independent EGO method and the mixed-EGO method is that $\mathbf{X}$ and t are sampled at two separate levels in the former method while $\mathbf{X}$ and t are sampled simultaneously in the latter method.

3.2 Initial Sampling. The initial samples $\mathbf{x}^s$ and t are generated to create an initial surrogate model for $Y_{\max}$. The commonly used sampling approaches include the random sampling, Latin hypercube sampling, and Hammersley sampling (HS) [31]. In this work, the HS method is used as it performs better in providing uniformity properties over a multidimensional space [32]. Samples are generated by the HS method in the [0, 1] domain. They are then transformed into samples of $\mathbf{X}$ and t according to their probability distributions using the inverse probability method. t is treated as if it was uniformly distributed.

Suppose that the dimension of $\mathbf{X}$ is n and that k initial samples are generated. The samples $\mathbf{x}^s$ are

$$\mathbf{x}^s = \left[\mathbf{x}^{(1)}; \mathbf{x}^{(2)}; \ldots; \mathbf{x}^{(k)}\right] = \begin{bmatrix} x_1^{(1)} & x_2^{(1)} & \cdots & x_n^{(1)} \\ x_1^{(2)} & x_2^{(2)} & \cdots & x_n^{(2)} \\ \vdots & \vdots & \ddots & \vdots \\ x_1^{(k)} & x_2^{(k)} & \cdots & x_n^{(k)} \end{bmatrix} \tag{12}$$

in which $\mathbf{x}^{(i)} = [x_1^{(i)}, x_2^{(i)}, \ldots, x_n^{(i)}]$ is the ith sample point. k initial samples of t are also generated along with those of $\mathbf{X}$. We then have the following combined initial samples:

$$[\mathbf{x}^s, \mathbf{t}^s] = \begin{bmatrix} x_1^{(1)} & x_2^{(1)} & \cdots & x_n^{(1)}, & t^{(1)} \\ x_1^{(2)} & x_2^{(2)} & \cdots & x_n^{(2)}, & t^{(2)} \\ \vdots & \vdots & \ddots & & \vdots \\ x_1^{(k)} & x_2^{(k)} & \cdots & x_n^{(k)}, & t^{(k)} \end{bmatrix} \tag{13}$$

We then call the limit-state function to obtain responses at the above sample points and build a mixed EGO model $Y = \hat{g}(\mathbf{X}, t)$ with respect to $\mathbf{X}$ and t. $Y = \hat{g}(\mathbf{X}, t)$ is called a mixed model

Table 3 Major procedure of the mixed-EGO based method

Step 1: Initial sampling
1. Generate initial samples $\mathbf{x}^s$ and $\mathbf{t}^s$
Step 2: Build initial extreme response model (Algorithm 3)
2. Build time-dependent surrogate model $Y = \hat{g}(\mathbf{X}, t)$
3. Solve for the maximum responses $Y_{\max}$ at $\mathbf{x}^s$ based on $Y = \hat{g}(\mathbf{X}, t)$ using the mixed EGO method
4. Build initial extreme response model $Y_{\max} = \hat{g}_{\max}(\mathbf{X})$
Step 3: Update extreme response model (Algorithm 4)
5. Adding new training points of $\mathbf{X}$ by the AK-MCS method [23]
6. Identify extreme values associated with the new training points using the mixed EGO method
7. Obtain final model $Y_{\max} = \hat{g}_{\max}(\mathbf{X})$
Step 4: Reliability analysis
8. Monte Carlo simulation based on $Y_{\max} = \hat{g}_{\max}(\mathbf{X})$

because it is a function of $\mathbf{X}$ and t. Then, the extreme value responses $\mathbf{y}^s_{\max}$ at $\mathbf{x}^s$ are identified based on the mixed EGO model that will be discussed in Sec. 3.3.

3.3 Construct Initial $Y_{\max} = \hat{g}_{\max}(\mathbf{X})$ With the Mixed EGO Model. This is step 2 of the mixed-EGO method in Table 3. With t, the EI in Eq. (4) is rewritten as

$$\mathrm{EI}\left(\mathbf{x}^{(i)}, t\right) = \left(\left(\mu(\mathbf{x}^{(i)}, t\right) - y_i^*\right)\Phi\left(\frac{\mu(\mathbf{x}^{(i)}, t) - y_i^*}{\sigma(\mathbf{x}^{(i)}, t)}\right) + \sigma\left(\mathbf{x}^{(i)}, t\right)\phi\left(\frac{\mu(\mathbf{x}^{(i)}, t) - y_i^*}{\sigma(\mathbf{x}^{(i)}, t)}\right) \quad (14)$$

where y_i^* is the current best solution (maximum response), and $\mu(\mathbf{x}^{(i)}, t)$ and $\sigma(\mathbf{x}^{(i)}, t)$ are the mean and standard deviation at $[\mathbf{x}^{(i)}, t]$, respectively.

The expressions of EI are the same as those for the independent EGO method and the mixed EGO model. The difference lies in the way of computing $\mu(\mathbf{x}^{(i)}, t)$ and $\sigma(\mathbf{x}^{(i)}, t)$. For the independent EGO method, $\mu(\mathbf{x}^{(i)}, t)$ and $\sigma(\mathbf{x}^{(i)}, t)$ are obtained from the one-dimensional Kriging model $Y = \hat{g}(t)$, which is constructed in the inner loop for t when $\mathbf{X}$ is fixed. For the mixed EGO model, they are computed from the Kriging model $Y = \hat{g}(\mathbf{X}, t)$, which is constructed when $\mathbf{X}$ and t vary simultaneously.

Once convergence is reached, the maximum responses with respect to $\mathbf{x}^s$ will be available. Then the initial model $Y_{\max} = \hat{g}_{\max}(\mathbf{X})$ can be built.

The algorithm (Algorithm 3) for the initial $Y_{\max} = \hat{g}_{\max}(\mathbf{X})$ is given as follows (Table 4):

In line 2, $\mathbf{x}^s$ contains initial samples used to construct $Y_{\max} = \hat{g}_{\max}(\mathbf{X})$, and $\mathbf{x}^s_t$ contains $\mathbf{x}^s$ and added samples of $\mathbf{X}$ for model $Y = \hat{g}(\mathbf{X}, t)$. In line 3, $\varepsilon_{\mathrm{EI}}$ is used as a convergence criterion for the maximum EI. In line 5, $\mathrm{EI}(\mathbf{x}^{(i)}, t)$ is computed by plugging $y^s_{\max}(i)$, $\mu_Y(\mathbf{x}^{(i)}, t)$ and $\mu_Y(\mathbf{x}^{(i)}, t)$, which are obtained from $Y = \hat{g}(\mathbf{X}, t)$, into Eq. (14). Note that in the mixed EGO model, all the sampled points of both $\mathbf{X}$ and t are used to identify the new training points of t. But in the independent EGO model, only the sampled points of t are used to update training points of t.

From the outputs of the mixed EGO model, we obtain the extreme values $\mathbf{y}^s_{\max}$ corresponding to the samples $\mathbf{x}^{(i)}$, $i = 1, 2, \ldots, k$. In Sec. 3.4, we discuss how to identify a new training point $\mathbf{x}^{(k+1)}$ and the associated $g_{\max}\left(\mathbf{x}^{(k+1)}\right)$.

Table 4 Detailed procedure of Algorithm 3

Algorithm 3: Mixed EGO model for initial $Y_{\max} = \hat{g}_{\max}(\mathbf{X})$

1 At initial samples points, compute $\mathbf{y}^s = [y^{(i)}]_{i=1,\ldots,k} = [g(\mathbf{x}^{(i)}, t^{(i)})]_{i=1,\ldots,k}$
2 Set $\mathbf{x}^s_t = \mathbf{x}^s$, $m = 1$, and the initial current best solution vector $\mathbf{y}^s_{\max} = \mathbf{y}^s$
3 **While** $\{m = 1\}$ **or** $\{I_{\max} < \varepsilon_{\mathrm{EI}}\}$ **do**
4 Construct Kriging model $Y = \hat{g}(\mathbf{X}, t)$ using $\{[\mathbf{x}^s_t, \mathbf{t}^s], \mathbf{y}^s\}$
5 Find a point with maximum EI:
$[\mathbf{x}^{(i_{\mathrm{EI}})}, t^{\mathrm{EI}}] = \arg\max_{i=1,2,\ldots,k}\{\max_{t\in[t_0,t_s]}\{\mathrm{EI}(\mathbf{x}^{(i)}, t)\}\}$, where $i_{\mathrm{EI}} \in [1, \ldots, k]$ and
$\mathrm{EI}(\mathbf{x}^{(i)}, t)$ is computed based on $Y = \hat{g}(\mathbf{X}, t)$; calculate
$I_{\max} = \mathrm{EI}(\mathbf{x}^{(i_{\mathrm{EI}})}, t^{\mathrm{EI}})/|\beta_{(\mathbf{x},t)}(1)|$.
6 Compute $y^{\mathrm{EI}} = g(\mathbf{x}^{(i_{\mathrm{EI}})}, t^{\mathrm{EI}})$
7 Update current best solution
$$y^s_{\max}(i_{\mathrm{EI}}) = \begin{cases} y^{\mathrm{EI}} & \text{if } y^{\mathrm{EI}} > y^s_{\max}(i_{\mathrm{EI}}) \\ y^s_{\max}(i_{\mathrm{EI}}) & \text{otherwise} \end{cases}$$
8 Update data points $\mathbf{x}^s_t = [\mathbf{x}^s_t; \mathbf{x}^{(i_{\mathrm{EI}})}]$, $\mathbf{t}^s = [\mathbf{t}^s; t^{\mathrm{EI}}]$, and $\mathbf{y}^s = [\mathbf{y}^s, y^{\mathrm{EI}}]$
9 $m = m + 1$
10 **End While**
11 Record $\mathbf{y}^s_{\max}$, $[\mathbf{x}^s_t, \mathbf{t}^s]$, and $\mathbf{y}^s$
12 Construct $Y_{\max} = \hat{g}_{\max}(\mathbf{X})$ using $\{\mathbf{x}^s, \mathbf{y}^s_{\max}\}$

3.4 Update $Y_{\max} = \hat{g}_{\max}(\mathbf{X})$ With AK–MCS and the Mixed EGO Model. The initial model of the extreme response $Y_{\max} = \hat{g}_{\max}(\mathbf{X})$ obtained above in general is not accurate. New training points of $\mathbf{X}$ should be added. As discussed in Sec. 3.1, it is desirable to generate more training points near or at the limit state. Several approaches are proposed for this purpose. For instance, the efficient global reliability analysis (EGRA) method [33] generates more training points adaptively near the limit state. Based on EGRA, an active learning approach called the AK–MCS method [23] is developed to further use the joint probability density of random variables for generating training points without using global optimization. Using the principle of AK–MCS, Wang and Wang later proposed a confidence enhanced sequential sampling approach [34]. Dubourg et al. integrated the importance sampling approach with the AK–MCS method [35] and further improved the efficiency. All of the above approaches are based on the Kriging model. Approaches based on other surrogate model techniques are also available. For example, support vector machines are used to generate explicit limit-state boundaries [36], and the same technique is also applied to identify disjoint failure domains and limit state boundaries for discontinuous responses [37]. The two methods are further improved by Basudhar and Missoum [38].

In this work, the AK–MCS method is employed to identify new training point $\mathbf{x}^{(k+1)}$ near the limit state of the extreme response $Y_{\max} = \hat{g}_{\max}(\mathbf{X})$. It has two advantages over the EGRA method: the joint probability density of random variables is considered during the sampling process, and it avoids global optimization in searching for new training points. A brief review of the AK–MCS method is given in the Appendix. Note that other sampling methods mentioned above can be used as well.

With the new training point $\mathbf{x}^{(k+1)}$ identified from AK–MCS, we can find the extreme response $g_{\max}\left(\mathbf{x}^{(k+1)}\right)$ to update the surrogate model for $Y_{\max}$. Obtaining $g_{\max}\left(\mathbf{x}^{(k+1)}\right)$ is equivalent to solving the following one-dimensional global optimization problem:

$$t^{(k+1)}_{\max} = \arg\max_{t\in[t_0,t_s]}\left\{y = g\left(\mathbf{x}^{(k+1)}, t\right)\right\} \quad (15)$$

To reduce the number of function calls, we still use the mixed EGO model presented in Sec. 3.3, and we also use the data set of $[\mathbf{x}^s_t, \mathbf{t}^s]$ and $\mathbf{y}^s$ obtained in Sec. 3.3. Algorithm 4 shows the details of finding $\mathbf{x}^{(k+1)}$ and $g_{\max}\left(\mathbf{x}^{(k+1)}\right)$ (Table 5).

In line 13, $\mathrm{EI}(\mathbf{x}^{\mathrm{new}}, t)$ is computed by plugging $y^{\mathrm{new}}_{\max}$, $\mu_Y(\mathbf{x}^{\mathrm{new}}, t)$, and $\sigma_Y(\mathbf{x}^{\mathrm{new}}, t)$, which are obtained from $Y = \hat{g}(\mathbf{X}, t)$, into Eq. (14). When the convergence criterion is satisfied, we obtain the surrogate model $Y_{\max} = \hat{g}_{\max}(\mathbf{X})$.

We then use MCS to calculate reliability. As $Y_{\max} = \hat{g}_{\max}(\mathbf{X})$ is accurate, so is the reliability calculated by MCS with a sufficiently large sample size. Note that MCS will no longer call the original limit-state state function.

We now have all the algorithms for the new method. Next, we put everything together and give the complete algorithm.

3.5 Summary of the Mixed EGO-Based Method. Combining Algorithms 3 and 4 yields the complete algorithm of the mixed EGO based method, or Algorithm 5 (Table 6).

4 Numerical Examples

In this section, three numerical examples are used to demonstrate the effectiveness of the proposed approach. Each of the examples is solved using the following four methods:

- Rice: the outcrossing rate method based on the Rice's formula and FORM [14,39].
- Independent EGO: the independent EGO method or the nested EGO [20]
- Mixed EGO: the proposed mixed EGO-based method
- MCS: the direct MCS method using the original limit-state function

Table 5 Detailed procedure of Algorithm 4

Algorithm 4: Sampling update

1 Set $r = 1$ and $\mathbf{x}^{\text{total}} = [\,]$
2 **While** $\{r = 1\}$ **or** $\{\text{Cov}_{pf} > 0.05\}$ **do**
3 Set $p = 1$
4 Generate n_{MCS} samples of $\mathbf{X}$, $\mathbf{x}_i^{\text{MCS}}, i = 1, 2, \ldots, n_{\text{MCS}}$; let $\mathbf{x}^{\text{total}} = [\mathbf{x}^{\text{total}}; \mathbf{x}^{\text{MCS}}]$
5 **While** $\{p = 1\}$ **or** $\{U_{\min} < \varepsilon_U\}$, where ε_U is the convergence criterion, **do**
6 Construct a Kriging model $Y_{\max} = \hat{g}_{\max}(\mathbf{X})$ using $\{\mathbf{x}^s, \mathbf{y}^s_{\max}\}$ and predict responses and their variances at $\mathbf{x}_i^{\text{MCS}}$ using $Y_{\max} = \hat{g}_{\max}(\mathbf{X})$
7 Compute $U(\mathbf{x}_i^{\text{MCS}})$ using Eq. (A1); identify a new training point by $\mathbf{x}^{\text{new}} = \arg \min\limits_{\mathbf{x} \in \mathbf{x}^{\text{MCS}}} \{\text{U}(\mathbf{x})\}$ and $U_{\min} = \text{U}(\mathbf{x}^{\text{new}})$
8 Generate a new time instant t_r from uniform distribution on $[t_0, t_s]$
9 Compute $y^{\text{MCS}} = g(\mathbf{x}^{\text{new}}, t_r)$; update $\mathbf{x}_t^s = [\mathbf{x}_t^s; \mathbf{x}^{\text{new}}]$, $\mathbf{t}^s = [\mathbf{t}^s; t_r]$, and $\mathbf{y}^s = [\mathbf{y}^s, y^{\text{MCS}}]$
10 Set $y^{\text{new}}_{\max} = y^{\text{MCS}}$ and $q = 1$
11 **While** $\{q = 1\}$ or $\{\max\limits_{t \in [t_0, t_s]} \text{EI}(\mathbf{x}^{\text{new}}, t) > \varepsilon_{\text{EI}}\}$ **do**
12 Construct $n + 1$ dimensional Kriging model $Y = \hat{g}(\mathbf{X}, t)$ using $\{[\mathbf{x}_t^s, \mathbf{t}^s], \mathbf{y}^s\}$
13 Find t^{EI} such that $t^{\text{EI}} = \max\limits_{t \in [t_0, t_s]} \{\text{EI}(\mathbf{x}^{\text{new}}, t)\}$, where $\text{EI}(\mathbf{x}^{\text{new}}, t)$ is computed based on $Y = \hat{g}(\mathbf{X}, t)$
14 Scale $\text{EI}(\mathbf{x}^{\text{new}}, t^{\text{EI}}) = \text{EI}(\mathbf{x}^{\text{new}}, t^{\text{EI}}) / |\beta_{(\mathbf{x},t)}(1)|$, where $\beta_{(\mathbf{x},t)}(1)$ is the first element of the trend coefficients of $Y = \hat{g}(\mathbf{X}, t)$ model
15 Compute $y^{\text{EI}} = g(\mathbf{x}^{\text{new}}, t^{\text{EI}})$
16 Update current best solution $y^{\text{new}}_{\max} = \begin{cases} y^{\text{EI}}, & \text{if } y^{\text{EI}} > y^{\text{new}}_{\max} \\ y^{\text{new}}_{\max}, & \text{otherwise} \end{cases}$
17 Update data points $\mathbf{x}_t^s = [\mathbf{x}_t^s; \mathbf{x}^{\text{new}}]$, $\mathbf{t}^s = [\mathbf{t}^s; t^{\text{EI}}]$, $\mathbf{y}^s = [\mathbf{y}^s, y^{\text{EI}}]$
18 $q = q + 1$
19 **End While**
20 Record $\mathbf{y}^s_{\max} = [\mathbf{y}^s_{\max}; y^{\text{new}}_{\max}]$, $\mathbf{x}^s = [\mathbf{x}^s; \mathbf{x}^{\text{new}}]$, $\mathbf{x}_t^s$, $\mathbf{t}^s$, and $\mathbf{y}^s$
21 $p = p + 1$
22 **End While**
23 Construct Kriging model of $Y_{\max} = \hat{g}_{\max}(\mathbf{X})$ using $\{\mathbf{x}^s, \mathbf{y}^s_{\max}\}$ and compute $\hat{p}_f$ by plugging $\mathbf{x}^{\text{total}}$ into $Y_{\max} = \hat{g}_{\max}(\mathbf{X})$
24 Compute $\text{Cov}_{pf} = \sqrt{(1 - \hat{p}_f)/(\hat{p}_f r n_{\text{MCS}})}$
25 $r = r + 1$
26 **End While**

Table 6 Detailed procedure of Algorithm 5

Algorithm 5: Complete algorithm

1) **Step 1: Initialization**
Generate initial samples $\mathbf{x}^s = [\mathbf{x}^{(1)}; \mathbf{x}^{(2)}; \ldots; \mathbf{x}^{(k)}]$ and $\mathbf{t}^s = [t^{(1)}; t^{(2)}; \ldots; t^{(k)}]$ using the Hammersley sampling method.

2) **Step 2: Build initial model $Y_{\max} = \hat{g}_{\max}(\mathbf{X})$ (Algorithm 3)**
a) Compute $\mathbf{y}^s = [y^{(i)}]_{i=1,\ldots,k} = [g(\mathbf{x}^{(i)}, t^{(i)})]_{i=1,\ldots,k}$
b) Set $\mathbf{x}_t^s = \mathbf{x}^s$, $m = 1$, and the initial current best solution vector $\mathbf{y}^s_{\max} = \mathbf{y}^s$
c) **While** $\{m = 1\}$ **or** $\{I_{\max} < \varepsilon_{\text{EI}}\}$ **do**
i) Construct an $n + 1$ dimensional Kriging model $Y = \hat{g}(\mathbf{X}, t)$ using $\{[\mathbf{x}_t^s, \mathbf{t}^s], \mathbf{y}^s\}$
ii) Find a point with maximum EI:
$[\mathbf{x}^{(i_{\text{EI}})}, t^{\text{EI}}] = \arg \max\limits_{i=1,2,\ldots,k} \{\max\limits_{t \in [t_0, t_s]} \{\text{EI}(\mathbf{x}^{(i)}, t)\}\}$, where $i_{\text{EI}} \in [1, \ldots, k]$;
calculate $I_{\max} = \text{EI}(\mathbf{x}^{(i_{\text{EI}})}, t^{\text{EI}}) / \left|\beta_{(\mathbf{x},t)}(1)\right|$.
iii) Compute $y^{\text{EI}} = g(\mathbf{x}^{(i_{\text{EI}})}, t^{\text{EI}})$
iv) Update current best solution
$y^s_{\max}(i_{\text{EI}}) = \begin{cases} y^{\text{EI}}, & \text{if } y^{\text{EI}} > y^s_{\max}(i_{\text{EI}}) \\ y^s_{\max}(i_{\text{EI}}), & \text{otherwise} \end{cases}$
v) Update data points $\mathbf{x}_t^s = [\mathbf{x}_t^s; \mathbf{x}^{(i_{\max})}]$, $\mathbf{t}^s = [\mathbf{t}^s; t^{\text{EI}}]$, $\mathbf{y}^s = [\mathbf{y}^s, y^{\text{EI}}]$
vi) $m = m + 1$
End While
d) Record $\mathbf{y}^s_{\max}$, $[\mathbf{x}_t^s, \mathbf{t}^s]$ and $\mathbf{y}^s$; Set $p = 1$.

3) **Step 3: Update $Y_{\max} = \hat{g}_{\max}(\mathbf{X})$ with AK-MCS and mixed EGO (Algorithm 4)**
Algorithm 4

4) **Step 4: Reliability Analysis**
Reliability analysis using $Y_{\max} = \hat{g}_{\max}(\mathbf{X})$

The other three methods are used to compare the accuracy and efficiency of the mixed EGO method.

4.1 A Nonlinear Mathematical Model.

A function of X and t is given in Eq. (16), where X is a random variable following a normal distribution $X \sim N(10, 0.5^2)$.

$$y(X, t) = \frac{1}{X^2 + 4} \sin(2.5X) \cos(t + 0.4)^2 \tag{16}$$

The time-dependent probability of failure is given by

$$p_f(t_0, t_s) = \Pr\{y(X, \tau) > 0.014, \quad \exists \tau \in [1, 2.5]\} \tag{17}$$

According to Eq. (8), $p_f(t_0, t_s)$ is equivalent to the following probability:

$$p_f(t_0, t_s) = \Pr\{Y_{\max} > 0.014\} \tag{18}$$

Before calculating reliability, we at first evaluate the mixed EGO model (or Algorithm 3) because it is the core component of the mixed EGO based method. We generate different numbers of initial samples of $\mathbf{X}$ and t. We then identify $\mathbf{y}^s_{\max}$ with respect to $\mathbf{x}^s$ using the existing independent EGO method and the mixed EGO method, respectively. The convergence criterion of the two methods is $\varepsilon_{\text{EI}} = 10^{-5}$. The numbers of samples of $\mathbf{X}$ are set to 10, 15, 18, and 20. The numbers of function evaluations (NOF) required for identifying $\mathbf{y}^s_{\max}$ for different numbers of initial samples of $\mathbf{X}$ are given in Table 7. The results show that the independent EGO calls the limit-state function 127 times to identify the extreme values when the sample size is 15 while the mixed EGO method only needs 59 function evaluations. The results for sample sizes of 10, 18, and 20 are similar. Figure 1 shows the values of $Y_{\max}$ (i.e., $\mathbf{y}^s_{\max}$) obtained from the two methods, as well as the true $Y_{\max}$, for the sample size of ten.

The results show that both models are accurate to extract the extreme responses. The number of function evaluations by the mixed EGO model is less than that by the independent EGO method. The former is therefore more efficient. This becomes more apparent when the number of samples of $\mathbf{X}$ becomes larger.

We now examine the performance of the mixed EGO based method for the time-dependent reliability analysis. We use the MCS solution as a benchmark for accuracy comparison. The percentage of error is computed by

$$\varepsilon\% = \frac{\left|p_f^{\text{MCS}} - p_f\right|}{p_f^{\text{MCS}}} \times 100\% \tag{19}$$

where p_f^{MCS} is from MCS that calls the original limit-state function, and p_f is from a non-MCS method. The results of reliability analysis are shown in Table 8.

The results show that the accuracy and efficiency of the mixed EGO based method are much better than the outcrossing rate method (Rice's formula) and the independent EGO method.

Table 7 NOF required for different number of samples of X

	NOF	
Number of samples of $\mathbf{X}$	Independent EGO	Mixed EGO
10	85	49
15	127	59
18	153	66
20	170	69

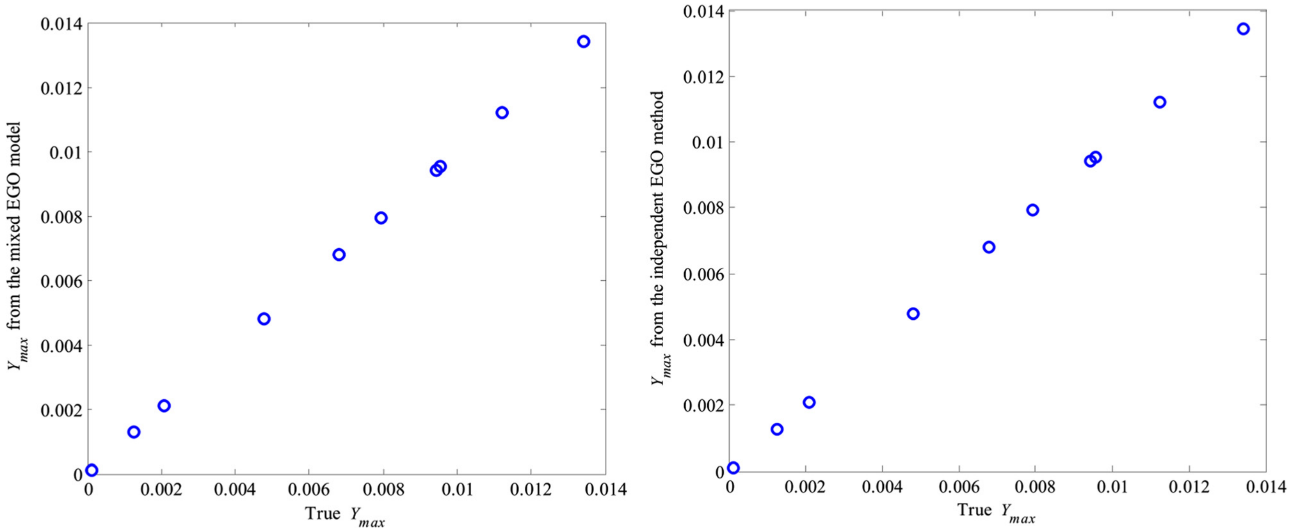

Fig. 1 $Y_{\max}$ **from independent EGO and mixed EGO and the true values**

Table 8 Results of Example 1

Method	NOF	$p_f(t_0, t_s)$ ($\times 10^{-4}$)	Error (%)
Rice	1017	0	100
Independent EGO	212	1.31	20.18
Mixed-EGO based	69	1.09	0
MCS	5×10^8	1.09	N/A

Table 9 Variables and parameters of Example 2

Variable	Mean	Standard deviation	Distribution
k_1 (N/m)	3×10^6	9×10^4	Normal
m_1 (kg)	1.6×10^4	2×10^2	Normal
k_2 (N/m)	8.5×10^4	2×10^3	Normal
m_2 (kg)	480	5	Normal
c_2 (Ns/m)	300	5	Normal

4.2 A Vibration Problem. A vibration problem as shown in Fig. 2 is modified from Ref. [40] by treating the stiffness of spring k_2, damping coefficient c_2, mass m_2, the stiffness of spring k_1, and mass m_1 as random variables. There are totally five random variables. The random variables are given in Table 9.

The amplitude of the vibration of mass m_1 subjected to force $f_0 \sin(\Omega t)$ is given by

$$q_{1\max} = f_0 \left(\frac{c_2^2\Omega^2 + \left(k_2 - m_2\Omega^2\right)^2}{c_2^2\Omega^2\left(k_1 - m_1\Omega^2 - m_2\Omega^2\right)^2 + \left(k_2 m_2\Omega^2 - \left(k_1 - m_1\Omega^2\right)\left(k_2 - m_2\Omega^2\right)\right)^2} \right)^{1/2} \quad (20)$$

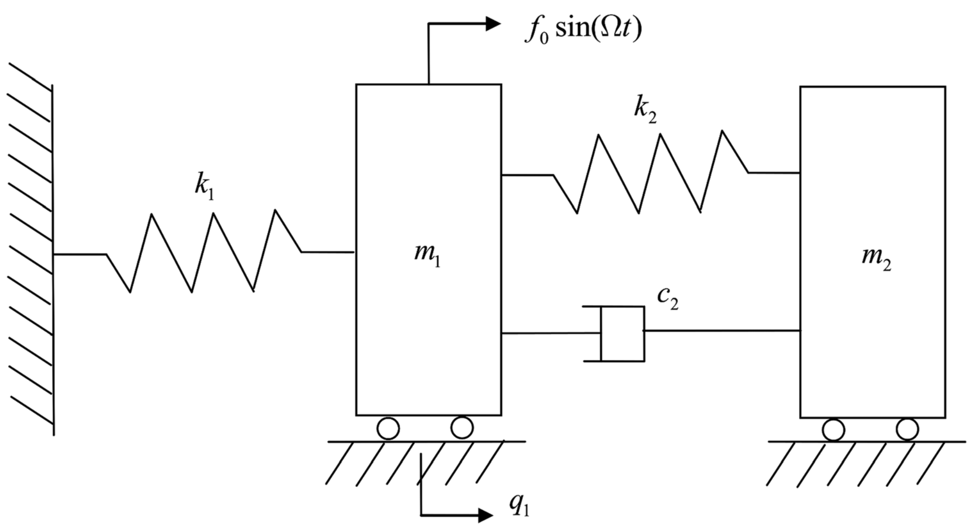

Fig. 2 A vibration problem

where Ω is the excitation frequency, which is considered as time, or $t = \Omega$.

Equation (20) can be nondimensionalized using a "static" deflection of the main system. The nondimensional displacement of m_1 is given by [40]

$$Y = g(\mathbf{X}, \Omega) = k_1\left(K_1/\left(K_2 + K_3^2\right)\right)^{1/2} \tag{21}$$

where $\mathbf{X} = [k_1, m_1]$, and K_i, $i = 1, 2, 3$, are given by

$$K_1 = \left(c_2^2\Omega^2 + \left(k_2 - m_2\Omega^2\right)^2\right) \tag{22}$$

$$K_2 = c_2^2\Omega^2\left(k_1 - m_1\Omega^2 - m_2\Omega^2\right)^2 \tag{23}$$

$$K_3 = \left(k_2 m_2\Omega^2 - \left(k_1 - m_1\Omega^2\right)\left(k_2 - m_2\Omega^2\right)\right) \tag{24}$$

Y is considered over a wide excitation frequency band, $8 \leq \Omega \leq 28$ (rad/s). Since Ω is treated as t, the period of time is $[8, 28]$ rad/s. A failure is defined as the event when Y is larger than 35. The probability of failure on $[8, 28]$ rad/s is given by

$$p_f(8, 28) = Pr\{g(\mathbf{X}, \Omega) > 35, \quad \exists\Omega \in [8, 28]\} \tag{25}$$

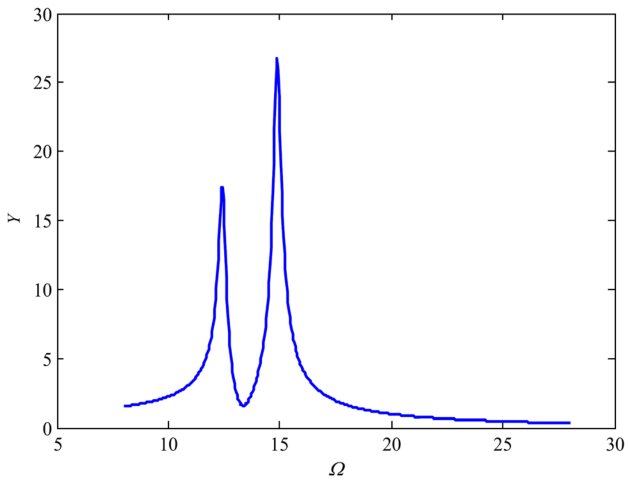

Fig. 3 One response *Y* at the mean value point of random variables

Table 10 Variables and parameters of Example 2

Method	NOF	$p_f(t_0, t_s)$ ($\times 10^{-2}$)	Error (%)
Rice		N/A	N/A
Independent EGO	3366	4.07	22.22
Mixed-EGO based	1378	3.43	3.00
MCS	2×10^8	3.33	N/A

Fig. 3 shows one response of Y at the means of random variables. It is highly nonlinear.

We use the independent EGO and the mixed EGO based methods to calculate the time-dependent probability of failure. Table 10 shows the results from different methods. Note that the Rice's formula based method is not applicable for this example as the response is highly nonlinear. The results show that the proposed mixed-EGO method is much more efficient than the independent EGO method. It should be noted that the vibration problem is employed as an example to verify the ability of the proposed method in solving highly nonlinear problem. Since the limit-state function is treated as a black box, the proposed method can be applied to other vibratory problems as well.

4.3 A Beam Subjected to Time-Variant Loading.

A corroded beam subjected to stochastic load as shown in Fig. 4 is used as the third example. This example is modified from Ref. [13].

A failure occurs when the stress of the beam is larger than the ultimate strength of the material. The time-dependent probability of failure is given by

$$p_f = Pr\{g(\mathbf{X}, Y(t), t) > 0, \quad \exists t \in [0, 35]\} \tag{26}$$

in which

$$g(\mathbf{X}, Y(t), t) = \left(F(t)L/4 + \rho_{st}a_0 b_0 L^2/8\right) - (a_0 - 2kt)(b_0 - 2kt)^2\sigma_u/4 \tag{27}$$

where $\mathbf{X} = [\sigma_u, a_0, b_0]$, $Y(t) = [F(t)]$, $\rho_{st} = 7.85 \times 10^4$ N, $k = 5 \times 10^{-5}$ m/year, and $L = 5$ m. Here, $F(t)$ is a stochastic loading presented by the spectral representation method [41] as follows:

$$F(t) = 6500 + \sum_{i=1}^{7}\xi_i\left(\sum_{j=1}^{7}\left(a_{ij}\sin(b_{ij}t + c_{ij})\right)\right) \tag{28}$$

where

$$a = \begin{bmatrix} 0.13 & 0.36 & 0.14 & 3.07 & 0.17 & 0.13 & 0.12 \\ 0.02 & 0.18 & 0.09 & 0.13 & 0.69 & 0.04 & 0.27 \\ 0.08 & 0.29 & 0.14 & 3.09 & 0.05 & 0.37 & 0.13 \\ 0.03 & 0.06 & 0.01 & 0.04 & 0.63 & 0.30 & 0.06 \\ 0.03 & 0.00 & 0.00 & 0.00 & 0.00 & 0.00 & 0.00 \\ 0.01 & 0.00 & 0.00 & 0.00 & 0.00 & 0.00 & 0.00 \\ 0.01 & 0.00 & 0.00 & 0.00 & 0.00 & 0.00 & 0.00 \end{bmatrix}$$

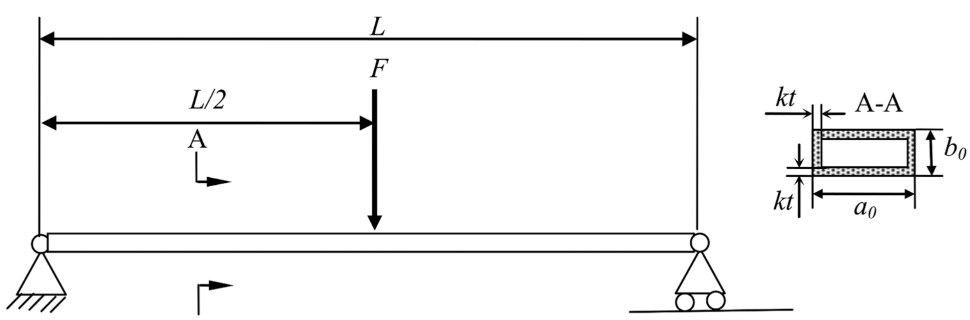

Fig. 4 Corroded beam subjected to stochastic loading

Table 11 Random variables of Example 3

Variable	Mean	Standard deviation	Distribution
σ_u (Pa)	2.4×10^8	2.4×10^7	Normal
a_0 (m)	0.2	0.01	Normal
b_0 (m)	0.04	4×10^{-3}	Normal
ξ_1	0	100	Normal
ξ_2	0	50	Normal
ξ_3	0	98	Normal
ξ_4	0	121	Normal
ξ_5	0	227	Normal
ξ_6	0	98	Normal
ξ_7	0	121	Normal

Table 12 Results of Example 3

Method	NOF	$p_f(t_0, t_s)$ $(\times 10^{-2})$	Error (%)
Rice	6501	2.85	5.94
Independent EGO	496	3.27	7.92
Mixed-EGO based	283	2.99	1.32
MCS	3×10^8	3.03	N/A

$$b = \begin{bmatrix} 0.06 & 0.31 & 0.15 & 0.28 & 0.24 & 0.44 & 0.48 \\ 0.38 & 0.15 & 0.40 & 0.06 & 0.42 & 0.09 & 0.01 \\ 0.10 & 0.33 & 0.03 & 0.29 & 0.11 & 0.26 & 0.38 \\ 0.28 & 0.07 & 0.59 & 0.55 & 0.42 & 0.23 & 0.29 \\ 0.52 & 0.00 & 0.00 & 0.00 & 0.00 & 0.00 & 0.00 \\ 0.77 & 0.00 & 0.00 & 0.00 & 0.00 & 0.00 & 0.00 \\ 0.91 & 0.00 & 0.00 & 0.00 & 0.00 & 0.00 & 0.00 \end{bmatrix}$$

$$c = \begin{bmatrix} 2.91 & -2.34 & -2.43 & -2.82 & -2.15 & 0.47 & 2.90 \\ -2.91 & 2.21 & -0.97 & 0.98 & -1.03 & -3.81 & -0.35 \\ 1.25 & 0.52 & 2.62 & 0.23 & 0.91 & -1.39 & -2.45 \\ 0.73 & 0.00 & -0.45 & -0.50 & 1.93 & -3.64 & -3.00 \\ 0.18 & 0.00 & 0.00 & 0.00 & 0.00 & 0.00 & 0.00 \\ -1.71 & 0.00 & 0.00 & 0.00 & 0.00 & 0.00 & 0.00 \\ -2.46 & 0.00 & 0.00 & 0.00 & 0.00 & 0.00 & 0.00 \end{bmatrix}$$

There are totally ten random variables, which are defined in Table 11.

The time-dependent probability of failure over [0, 35] years is calculated by aforementioned four methods, and the results are given in Table 12.

The results show that the mixed EGO-based method is much more efficient and accurate than the independent EGO method and the Rice's formula based method.

5 Conclusion

The distribution of the extreme value of a time-dependent limit-state function is required to evaluate the reliability defined within a period of time. The extreme value may be highly nonlinear with a multimodal distribution with respect to random input variables. For this reason, existing approximation methods, such as FORM, SORM, and the upcrossing method, may produce large errors. Using MCS based on the surrogate model of the extreme response becomes more practical.

This work develops a new reliability method that can efficiently and accurately construct surrogate models of extreme responses. The EGO is employed, and the sample points of input random variables and time are simultaneously generated. With this treatment, the new method is much more efficient than the existing method where the two sets of samples are generated independently in two nested loops. The surrogate model from the new method is accurate near or at the limit state, and its accuracy in other area is not important for the reliability assessment. This is another reason for the high efficiency. After the surrogate model is available, the reliability can then be easily estimated by MCS, which will not call the original limit-state function any more.

As indicated in Sec. 4.2, where t is the frequency, instead of a time factor, the proposed method can be used for limit-state functions with random input variables $\mathbf{X}$ and a general interval variable t. The latter may not necessarily be a time factor. The reliability produced by the proposed method becomes the worst-case reliability with respect to the interval variable.

The new method is based on the Kriging model, and during the sampling and model updating process, the Kriging model is called repeatedly. The computational cost of calling the Kriging model is minor or moderate compared to that of calling a limit-state function whose evaluation may be computationally expensive.

Acknowledgment

This material is based upon work supported by the National Science Foundation through Grant No. CMMI 1234855. The support from the Intelligent Systems Center (ISC) at the Missouri University of Science and Technology is also acknowledged.

Appendix: Review of the AK–MCS Method

The AK–MCS method [23] is developed based on the EGRA method [33]. In the AK–MCS method, the Kriging model is combined with MCS to adaptively update training points near or at the limit state. A Kriging model $G = \hat{f}(\mathbf{x})$ is constructed with initial training points $\{\mathbf{x}, \mathbf{G}\}$. In order to identify a potential "dangerous" point (i.e., the new training point), which may cause the change of the sign of the response variable, one can use a learning function defined by [23]

$$U(\mathbf{x}^{\mathrm{MCS}}) = \frac{|\mu_G(\mathbf{x}^{\mathrm{MCS}})|}{\sigma_G(\mathbf{x}^{\mathrm{MCS}})} \tag{A1}$$

where $\mathbf{x}^{\mathrm{MCS}}$ is a group of samples drawn from the distributions of random input variables, $\mu_G(\mathbf{x}^{\mathrm{MCS}})$ is the prediction form the Kriging model $G = \hat{f}(\mathbf{x})$, and $\sigma_G^2(\mathbf{x}^{\mathrm{MCS}})$ is the variance of the prediction. Note that the population of MCS samples is used to consider the joint probability density information of random variables and avoid the complicated global optimization used in the EGRA method.

Table 13 Detailed procedure of Algorithm 6

Algorithm 6: Algorithm of AK-MCS

Set $q = 1$ and $\mathbf{x}^{\mathrm{total}} = [\ ]$
While $\{q = 1\}$ **or** $\{\mathrm{Cov}_{pf} > 0.05\}$ **do**
  Set $p = 1$
  Generate n_{MCS} samples of $\mathbf{X}$, $\mathbf{x}_i^{\mathrm{MCS}}, i = 1, 2, \ldots, n_{\mathrm{MCS}}$; let $\mathbf{x}^{\mathrm{total}} = [\mathbf{x}^{\mathrm{total}}; \mathbf{x}^{\mathrm{MCS}}]$
  While $\{p = 1\}$ **or** $\{U_{\min} < \varepsilon_U\}$ **do**
    Construct a Kriging model of $G = \hat{f}(\mathbf{X})$ using initial training points$\{\mathbf{x}, \mathbf{G}\}$ and obtain the predictions and variances by plugging $\mathbf{x}_i^{\mathrm{MCS}}$ into $G = \hat{f}(\mathbf{X})$
    Identify new training point by $\mathbf{x}^{\mathrm{new}} = \arg \min_{\mathbf{x} \in \mathbf{x}^{\mathrm{MCS}}} \{\mathrm{U}(\mathbf{x})\}$ and $U_{\min} = \mathrm{U}(\mathbf{x}^{\mathrm{new}})$
    Compute $y^{\mathrm{new}} = f(\mathbf{x}^{\mathrm{new}})$; Update $\mathbf{x} = [\mathbf{x}; \mathbf{x}^{\mathrm{new}}]$ and $\mathbf{g} = [\mathbf{g}, y^{\mathrm{new}}]$
  End While
  Compute $\hat{p}_f$ by plugging $\mathbf{x}^{\mathrm{total}}$ into $G = \hat{f}(\mathbf{X})$
  Compute Cov_p_f with Cov_$p_f = \sqrt{(1 - p_f)/(p_f q n_{\mathrm{MCS}})}$
  $q = q + 1$
End While

Then, a new training point is identified by minimizing $U(\mathbf{x}^{\mathrm{MCS}})$. A stopping criterion ε_U is defined as $\min\{U(\mathbf{x})\} \geq \varepsilon_U$ [23]. After the convergence is achieved, the probability of failure p_f is estimated by plugging current available samples $\mathbf{x}^{\mathrm{total}}$ into the surrogate model, where $\mathbf{x}^{\mathrm{total}} = [\mathbf{x}^{\mathrm{total}}; \mathbf{x}^{\mathrm{MCS}}]$ is used to store total samples for the current iteration. Then the coefficient of variation of probability of failure Cov_{pf} is checked by

$$\mathrm{Cov}_{pf} = \sqrt{(1 - p_f)/(p_f N_{\mathrm{MCS}})} \tag{A2}$$

where N_{MCS} is the total number of samples in $\mathbf{x}^{\mathrm{total}}$.

If $\mathrm{Cov}_{pf} > 0.05$, continue above procedure. Otherwise, stop and obtain the approximated p_f. The general algorithm of the AK–MCS summarized in Table 13.

References

[1] Du, X., and Hu, Z., 2012, "First Order Reliability Method With Truncated Random Variables," ASME J. Mech. Des., **134**(9), p. 091005.
[2] Zhang, J., and Du, X., 2010, "A Second-Order Reliability Method With First-Order Efficiency," ASME J. Mech. Des., **132**(10), p. 101006.
[3] Li, J., Mourelatos, Z., and Singh, A., 2012, "Optimal Preventive Maintenance Schedule Based on Lifecycle Cost and Time-Dependent Reliability," SAE Int. J. Mater. Manuf., **5**(1), pp. 87–95.
[4] Singh, A., Mourelatos, Z. P., and Li, J., 2010, "Design for Lifecycle Cost Using Time-Dependent Reliability," ASME J. Mech. Des., **132**(9), p. 091008.
[5] Singh, A., Mourelatos, Z. P., and Nikolaidis, E., 2011, "An Importance Sampling Approach for Time-Dependent Reliability," ASME Paper No. DETC2011-47200.
[6] Rice, S. O., 1945, "Mathematical Analysis of Random Noise," Bell Syst.Tech. J., **24**(1), pp. 146–156.
[7] Lindgren, G., 1984, "Extremal Ranks and Transformation of Variables or Extremes of Functions of Multivariate Gaussian Processes," Stochastic Process Appl., **17**(2), pp. 285–312.
[8] Breitung, K., 1984, "Asymptotic Crossing Rates for Stationary Gaussian Vector Processes," Department of Mathematics and Statistics, University of Lund, Lund, Sweden, Technical Report No. 1.
[9] Breitung, K., 1988, "Asymptotic Crossing Rates for Stationary Gaussian Vector Processes," Stochastic Process Appl., **13**(2), pp. 195–207.
[10] Ditlevsen, O., 1983, "Gaussian Outcrossings From Safe Convex Polyhedrons," J. Eng. Mech., **109**(1), pp. 127–148.
[11] Hagen, O., and Tvedt, L., 1991, "Vector Process Out-Crossing as Parallel System Sensitivity Measure," J. Eng. Mech., **117**(10), pp. 2201–2220.
[12] Hagen, O., and Tvedt, L., 1992, "Parallel System Approach for Vector Out-Crossing," ASME J. Offshore Mech. Arct. Eng., **114**(2), pp. 122–128.
[13] Andrieu-Renaud, C., Sudret, B., and Lemaire, M., 2004, "The PHI2 Method: A Way to Compute Time-Variant Reliability," Reliab. Eng. Syst. Saf., **84**(1), pp. 75–86.
[14] Hu, Z., and Du, X., 2012, "Reliability Analysis for Hydrokinetic Turbine Blades," Renewable Energy, **48**(1), pp. 251–262.
[15] Vanmarcke, E. H., 1975, "On the Distribution of the First-Passage Time for Normal Stationary Random Processes," ASME J. Appl. Mech., **42**(1), pp. 215–220.
[16] Madsen, P. H., and Krenk, S., 1984, "Integral Equation Method for the First-Passage Problem in Random Vibration," ASME J. Appl. Mech., **51**(3), pp. 674–679.
[17] Hu, Z., and Du, X., 2013, "Time-Dependent Reliability Analysis With Joint Upcrossing Rates," Struct. Multidiscip. Optim., **48**(5), pp. 893–907.
[18] Hu, Z., Li, H., Du, X., and Chandrashekhara, K., 2012, "Simulation-Based Time-Dependent Reliability Analysis for Composite Hydrokinetic Turbine Blades," Struct. Multidiscip. Optim., **47**(5), pp. 765–781.
[19] Bichon, B. J., Eldred, M. S., Swiler, L. P., Mahadevan, S., and McFarland, J. M., 2007, "Multimodal Reliability Assessment for Complex Engineering Applications Using Efficient Global Optimization," AIAA Paper No. AIAA-2007-1946.
[20] Wang, Z., and Wang, P., 2012, "A Nested Extreme Response Surface Approach for Time-Dependent Reliability-Based Design Optimization," ASME J. Mech. Des., **134**(12), p. 121007.
[21] Jones, D. R., Schonlau, M., and Welch, W. J., 1998, "Efficient Global Optimization of Expensive Black-Box Functions," J. Global Optim., **13**(4), pp. 455–492.
[22] Chen, J. B., and Li, J., 2007, "The Extreme Value Distribution and Dynamic Reliability Analysis of Nonlinear Structures With Uncertain Parameters," Struct. Saf., **29**(2), pp. 77–93.
[23] Echard, B., Gayton, N., and Lemaire, M., 2011, "AK–MCS: An Active Learning Reliability Method Combining Kriging and Monte Carlo Simulation," Struct. Saf., **33**(2), pp. 145–154.
[24] Hu, Z., and Du, X., 2013, "A Sampling Approach to Extreme Value Distribution for Time-Dependent Reliability Analysis," ASME J. Mech. Des., **135**(7), p. 071003.
[25] Hu, Z., and Du, X., 2014, "Lifetime Cost Optimization With Time-Dependent Reliability," Eng. Optim., **46**(10), pp. 1389–1410.
[26] Grogan, J. A., Leen, S. B., and Mchugh, P. E., 2013, "Optimizing the Design of a Bioabsorbable Metal Stent Using Computer Simulation Methods," Biomaterials, **34**(33), pp. 8049–8060.
[27] Lockwood, B., and Mavriplis, D., 2013, "Gradient-Based Methods for Uncertainty Quantification in Hypersonic Flows," Comput. Fluids, **85**(1), pp. 27–38.
[28] Raghavan, B., and Breitkopf, P., 2013, "Asynchronous Evolutionary Shape Optimization Based on High-Quality Surrogates: Application to an Air-Conditioning Duct," Eng. Comput., **29**(4), pp. 467–476.
[29] Steponavičе, I., Ruuska, S., and Miettinen, K., 2014, "A Solution Process for Simulation-Based Multiobjective Design Optimization With an Application in the Paper Industry," Comput. Aided Des., **47**, pp. 45–58.
[30] Lophaven;, S. N., Nielsen;, H. B., and Søndergaard, J., 2002, "DACE—A MATLAB Kriging Toolbox," Technical University of Denmark, Lyngby, Denmark.
[31] Chen, W., Tsui, K.-L., Allen, J. K., and Mistree, F., 1995, "Integration of the Response Surface Methodology With the Compromise Decision Support Problem in Developing a General Robust Design Procedure," 1995 ASME Design Engineering Technical Conference, pp. 485–492.
[32] Hosder, S., Walters, R. W., and Balch, M., 2007, "Efficient Sampling for Non-Intrusive Polynomial Chaos Applications With Multiple Uncertain Input Variables," 48th AIAA/ASME/ASCE/AHS/ASC Structures, Structural Dynamics and Materials Conference, Honolulu, HI, Apr. 23–25, pp. 2946–2961.
[33] Bichon, B. J., Eldred, M. S., Swiler, L. P., Mahadevan, S., and McFarland, J. M., 2008, "Efficient Global Reliability Analysis for Nonlinear Implicit Performance Functions," AIAA J., **46**(10), pp. 2459–2468.
[34] Wang, Z., and Wang, P., 2014, "A Maximum Confidence Enhancement Based Sequential Sampling Scheme for Simulation-Based Design," ASME J. Mech. Des., **136**(2), p. 021006.
[35] Dubourg, V., Sudret, B., and Deheeger, F., 2013, "Metamodel-Based Importance Sampling for Structural Reliability Analysis," Probab. Eng. Mech., **33**, pp. 47–57.
[36] Basudhar, A., and Missoum, S., 2008, "Adaptive Explicit Decision Functions for Probabilistic Design and Optimization Using Support Vector Machines," Comput. Struct., **86**(19), pp. 1904–1917.
[37] Basudhar, A., Missoum, S., and Harrison Sanchez, A., 2008, "Limit State Function Identification Using Support Vector Machines for Discontinuous Responses and Disjoint Failure Domains," Prob. Eng. Mech., **23**(1), pp. 1–11.
[38] Basudhar, A., and Missoum, S., 2010, "An Improved Adaptive Sampling Scheme for the Construction of Explicit Boundaries," Struct. Multidiscip. Optim., **42**(4), pp. 517–529.
[39] Zhang, J., and Du, X., 2011, "Time-Dependent Reliability Analysis for Function Generator Mechanisms," ASME J. Mech. Des., **133**(3), p. 031005.
[40] Zang, C., Friswell, M. I., and Mottershead, J. E., 2005, "A Review of Robust Optimal Design and Its Application in Dynamics," Comput. Struct., **83**(4–5), pp. 315–326.
[41] Li, C.-C., and Der Kiureghian, A., 1993, "Optimal Discretization of Random Fields," J. Eng. Mech., **119**(6), pp. 1136–1154.